ELSEVIER

Journal of Alloys and Compounds 430 (2007) 142–148

Journal of ALLOYS AND COMPOUNDS

www.elsevier.com/locate/jallcom

Structural phase transition in the Hf–Ni system studied by *ab initio* calculation and ion beam mixing

H.F. Yan, H.B. Guo, B.X. Liu *

Advanced Materials Laboratory, Department of Materials Science and Engineering, Tsinghua University, Beijing 100084, China

Received 13 January 2006; received in revised form 27 April 2006; accepted 28 April 2006
Available online 12 June 2006

Abstract

Hafnium films with the respective thicknesses of 100, 200, 300, 400 Å were examined by transmission electron microscopy and were shown to deposit with an hcp structure, then transformed into an fcc structure after being irradiated by 200 KeV xenon ions at 77 K. The first principles calculation showed the cohesive energies per atom of the hcp and fcc structures of Hf were extremely close, which was probably responsible for the observed hcp-to-fcc structural transition upon irradiation. Meanwhile, a deposited Hf–Ni–Hf sandwich-structured film with an overall composition around $Ni_{25}Hf_{75}$ was identified to consist of two fcc structures and later transformed into a uniform fcc structure upon irradiation, which is also confirmed by *ab initio* calculation that the fcc-type ($L1_2$) crystalline phase was more likely to be formed than the hcp-type for a possible Hf-rich $Ni_{25}Hf_{75}$ alloy.

Keywords: Ion beam mixing; *Ab initio* calculation; The Hf–Ni system; Structural phase transition

1. Introduction

Since the early 1980s, a scheme of ion beam mixing (IBM) has been introduced and proved to be a powerful means for producing metastable alloys as well as for studying the structural stability of the metastable crystalline alloys [1]. Generally according to the atomic collision theory, the IBM can provide additional energy to trigger an atomic collision cascade in the multilayered films, resulting in a mixture in a highly energetic state, and later, during the relaxation period (lasting only for 10^{-10}–10^{-9} s) immediately after the atomic collision cascade, the mixture could reside at one of the possible non-equilibrium states since there is no enough time for atomic diffusion, nucleation, growth or time consuming phase transitions [1,2]. Thus, the IBM scheme has extensively been employed for studying the structural phase transition and metastable phase formation. For example, He et al. [3] have observed interesting structural transition in the nano-sized Pd–Ru multilayered films by IBM. Li et al. [4] have reported the formation of two overlapping fcc lattices in the AgCo and AgNi multilayered films by IBM. These results show that the scheme of IBM is capable of revealing some new structural phase transitions, which have not been observed by other equilibrium materials processing methods in the binary metal systems.

Along with the experimental advances, theoretical calculation methods have also been widely employed to clarify the physical origin responsible for those observed structural phase transition upon IBM as well as to predict the possible metastable states in the transitional metal systems. For instance, under the framework of Miedema's model [5], a semi-empirical approach has been proposed to explain or predict the formation of the metastable solid phases. Molecular dynamics (MD) simulations have been performed to reveal the atomistic mechanism of the solid-state interfacial reaction in the equilibrium miscible as well as immiscible metal–metal multilayered films at an atomic scale. In recent years, first principles calculations have been employed to approach a better understanding at a depth of electronic structure of materials concerning the metastability, i.e., the structural stability of the metastable solid phases, in the transition metal binary systems.

In the present study, pure Hf as well as the Hf–Ni system was selected to investigate the structural stabilities of the Hf and Hf–Ni alloy phases by the scheme of IBM. Although the structural phase transitions of both systems have ever been stud-

* Corresponding author. Tel.: +86 10 6277 2557; fax: +86 10 6277 1160.
E-mail address: dmslbx@tsinghua.edu.cn (B.X. Liu).

0925-8388/$ – see front matter © 2006 Elsevier B.V. All rights reserved.
doi:10.1016/j.jallcom.2006.04.071

ied by some other researchers either through IBM experiments or MD simulations at an atomic scale, e.g. Jin et al. [6] had ever observed the hcp-to-fcc structural phase transition under IBM in the pure Hf film with the individual thickness of 400 Å and discussed this structural phase transition based on the semi-empirical Miedema's model and Li. et al. [7] executed the MD simulation using a proven realistic *n*-body Hf–Ni potential to find the hcp-to-fco martensitic transformation in the Hf–Ni system. It seemed that the structural phase transitions in such a system were commonly inclined to happen and therefore, in the present work, we dedicated to investigate such a phenomenon of pure Hf films with different thicknesses and that of the Hf–Ni system with a sandwich structure with the aid of *ab initio* calculation and IBM. The *ab initio* calculations were employed to calculate the total energies of some specific structures of the systems at the electronic level and then to confirm the structural stabilities in IBM experiment. We hope that the combination of *ab initio* calculation and IBM experiment could help us a better understanding on the detailed structural stabilities of the Hf and the Hf–Ni alloy phases.

2. Calculation methods and experimental procedure

2.1. First principles calculation

The first principles calculation is carried out based on the well-established Vienna *ab initio* simulation package (VASP) [8–10], The calculation is conducted in plane-wave basis, using fully nonlocal Vanderbilt-type ultrasoft pseudopotentials to describe the electron–ion interaction, [11] which allows the use of a moderate cutoff for the construction of the plane-wave basis for the transition metals. The exchange and correlation items are described by the generalized-gradient approximation (GGA) proposed by Perdew and Wang [12]. The integration in the Brillouin zone is done on special k points determined according to the Monkhorst-Pack scheme [13]. In studying the stability of Hf metastable crystalline phases, we selected the hcp and fcc structures of Hf in the calculations. In the calculation of $Ni_{25}Hf_{75}$ metastable structures, some representative structures, i.e., A15, $L1_2$, $D0_9$, $D0_{22}$ and $D0_{19}$ structures were selected to test their relative stabilities. In order to compare those estimated structures with the mechanical mixture of 75% fcc-Hf and 25% fcc-Ni, we also calculated the total energy of the pure fcc-Ni to figure out the total energy of the mixture.

2.2. Experimental procedure

In the present study, two sets of the samples were prepared and studied. One was for pure Hf system. To investigate the structural transition in the pure Hf films with different thicknesses, four samples with 100, 200, 300 and 400 Å thick, respectively, were prepared in an electron-gun evaporation system by depositing pure hafnium (99.9%) onto NaCl single crystal substrates, which were cooled by running water (283 K) during deposition. The other is for the Hf–Ni system. The samples were prepared with a sandwich structure (one Ni layer between two Hf layers) with the different relative thicknesses of the individual Ni and Hf layers. The total thickness of the Hf–Ni multilayered samples was fixed to be 40 nm, according to the calculated ion range based on the TRIM program [14]. The designed Hf–Ni sandwich-structured film was prepared by depositing pure Hafnium (99.9%) firstly onto NaCl single crystals, then depositing an individual Ni layers on it, and at last depositing another pure Hafnium layer in an ultrahigh-vacuum (UHV) e-gun evaporation system with a background vacuum level on the order of 10^{-6} Pa. During deposition, the vacuum level was higher than 3.0×10^{-4} Pa. The deposition rate for both Ni and Hf was controlled at 0.5 Å/s, and during deposition, the sample holders were cooled by the running water of about 10 °C. Rutherford backscattering spectrometry (RBS) was employed to confirm the sandwich structure of the Ni–Hf multilayer with 2.0 MeV He ions at a 165° scattering angle by measuring the depth profile of two constituent elements. Following these specifications, two sets of samples were designed and their features are listed in Table 1. The as-deposited films were then subjected to 200 keV xenon ion irradiation to doses ranging from 5×10^{14} to 9×10^{15} Xe^+/cm^2 in an implanter with a base vacuum level on the order of 10^{-4} Pa. During irradiation, the sample holders were cooled by liquid nitrogen and the ion current density was controlled to be less than 1 $\mu A/cm^2$ to avoid overheating. Under such precautions, the temperature of the films was estimated to be around 77 K. The vacuum level during irradiation was better than 5×10^{-4} Pa. For structural characterization, the Hf and Hf–Ni films were removed from the NaCl substrates by de-ionized water and placed onto the Cu grids for the transmission electron microscopy (TEM) observation and selected area diffraction (SAD) analysis to identify the structures in the as-deposited states as well as the resultant Hf and Hf–Ni films upon irradiation by 200 keV xenon ions. The lattice constants of the resultant Hf and Hf–Ni crystalline phases could be determined by the corresponding SAD patterns with the errors around 5%. To obtain a precise value of the Hf and Ni content in the films, the PLASMA-SPEC-I inductive coupled plasma (ICP) atomic emission spectrum was employed and its measuring error was about 6%.

Table 1
Design of pure Hf films and the Ni–Hf sandwich-structured film

Sample	Thickness (Å)		Layered structure
	Hf	Ni	
Hafnium	100		Hf
	200		Hf
	300		Hf
	400		Hf
Ni–Hf	175	50	Hf–Ni–Hf

3. Results and discussion

3.1. Ab initio calculation results

We first present the calculation results for the hcp and fcc structures of the pure Hf. The total energy was calculated as a function of the lattice constant for the hcp and fcc structures, respectively, and Fig. 1 exhibits the two calculated curves showing the correlation of the total energy versus average atomic volume. Table 2 lists the calculated equilibrium cohesive properties of both hcp and fcc structures. One sees from Fig. 1 that the difference between the minimum total energies of the hcp and fcc structures is very small, and from Table 2, the cohesive energy difference between the two structures is about 0.07 eV/atom, i.e., 0.7%. The calculated results suggest that both hcp and fcc structures are possible to be formed, whenever the formation condition could provide the relevant energy to have the related structural phase transition taking place. Moreover, as the fcc and hcp structures are very much alike in their atomic configurations, it is quite reasonable that the total energies of the fcc and hcp structures are very close.

Ab initio calculations are also performed for several simple crystalline structures, i.e, A15, $L1_2$, $D0_{22}$, $D0_9$, $D0_{19}$ struc-

Table 2
The calculated equilibrium cohesive properties (lattice constant a and c/a, atomic volume V, cohesive energy E_{min}) of hcp and fcc structures of hafnium and of A15, $L1_2$, $D0_9$, $D0_{22}$ and $D0_{19}$ structures of $Ni_{25}Hf_{75}$

	Hf		$Ni_{25}Hf_{75}$				
	hcp	fcc	A15	$L1_2$	$D0_9$	$D0_{19}$	$D0_{22}$
a (Å)	3.20	4.51	5.37	4.24	4.86	2.63	4.93
c/a	1.58					1.63	
V (Å^3/atom)	22.5206	22.9323	19.4030	19.0785	28.7514	25.8042	18.9113
E_{min} (eV/atom)	−9.8029	−9.7333	−8.7894	−8.7100	−7.2752	−7.0998	−8.5333

tures at an alloy composition of $Ni_{25}Hf_{75}$, which represents a possible metastable Hf-rich Hf–Ni alloy. Accordingly, the correlations between the total energy and average atomic volume for the $Ni_{25}Hf_{75}$ alloys in different structures are obtained and displayed in Fig. 2. One sees clearly from the figure that the possible $Ni_{25}Hf_{75}$ alloys in $L1_2$ and A15 structures (both are fcc types) have the relatively lowest total energies among the calculated structures and the total energy difference between $L1_2$ and A15 is very small, i.e., 0.0794 eV. In addition, the total energies of both $L1_2$ and $A1_5$ were lower than that of the mixture with 75% fcc-Hf and 25% fcc-Ni (represented by the straight dash-dot-dotted line in the figure), i.e., both the structures were more inclined to be formed than the mechanical mixture. It is worthwhile to be mentioned that among the calculated structures, the possible $Ni_{25}Hf_{75}$ alloy in $D0_{19}$ (hexagonal type) structure has the highest total energy, which indicated that the hexagonal type crystal lattice could not be stable in the $Ni_{25}Hf_{75}$ alloys. The calculated properties for the A15, $L1_2$, $D0_9$, $D0_{22}$ and $D0_{19}$ structures at the alloy composition of $Ni_{25}Hf_{75}$ are all listed in Table 2.

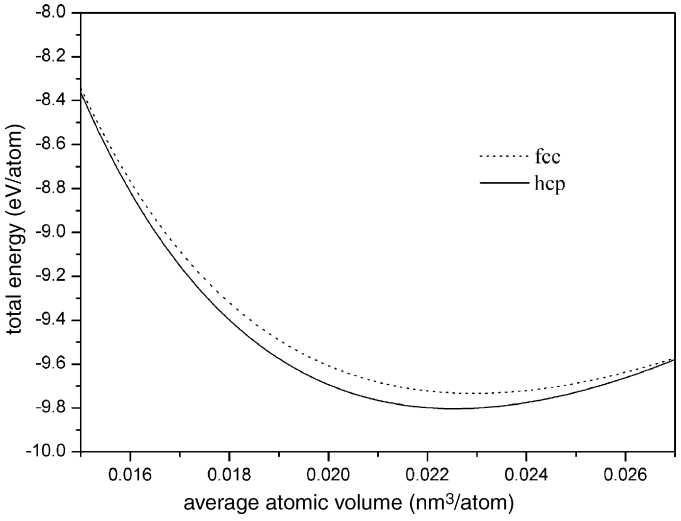

Fig. 1. The calculated total energy vs. the average atomic volume for the fcc and hcp structures of Hf.

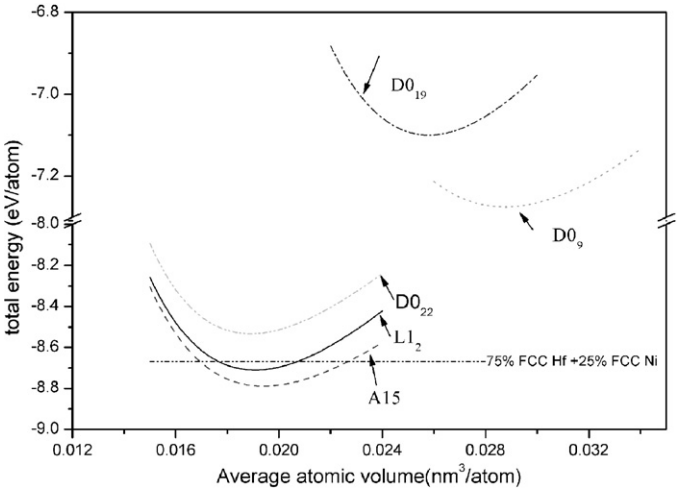

Fig. 2. The calculated total energy vs. the average atomic volume for the $Ni_{25}Hf_{75}$ phase with different structures.

3.2. The hcp to fcc structural phase transition in Hf

Fig. 3 (a) and (b) showed the SAD pattern and TEM bright-field image for an as-deposited Hf film with the thickness of 40 nm, respectively. Table 3 lists the crystallographic indexing results from the observed SAD pattern of the Hf film, which was identified to be an hcp structure. Besides this, the structures of the as-deposited pure Hf films with other thicknesses of 10, 20 and 30 nm, respectively were all identified to be the same

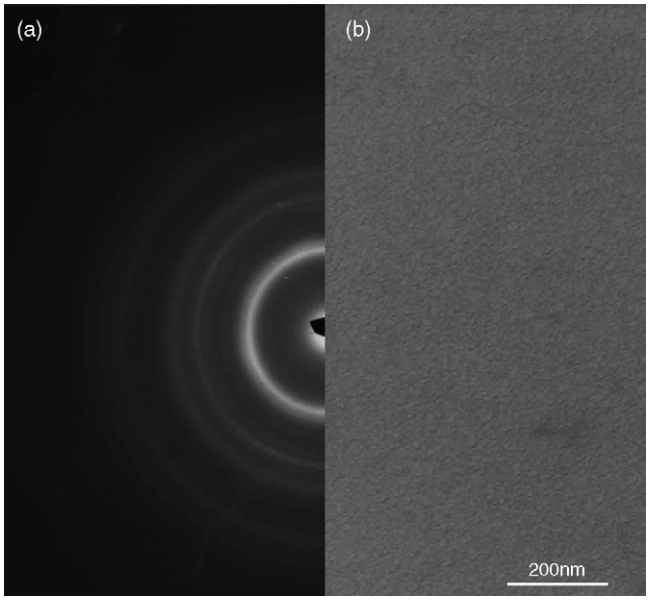

Fig. 3. (a) The SAD pattern of an hcp structure. (b) The corresponding TEM bright-field image of the as-deposited pure Hf film.

Table 3
Indexing of the hcp structure in the as-deposited pure Hf film

D_{exp} (Å)	hkl	D_{cal} (Å)
2.45	101	2.44
1.89	102	1.89
1.61	110	1.59
1.53	111	1.52
1.32	201	1.33
1.24	202	1.22

$a = 3.19$ Å; $c/a = 1.62$.

hcp structure. The lattice constants of the hcp structures were calculated to be $a = 3.19$ Å and $c/a = 1.62$ within the error around 5% for the as-deposited Hf film, which are very close to those of the pure bulk Hf (α-Hf) ($a = 3.198$ Å and $c/a = 1.56$, according to the JCPDS card).

Fig. 4(a) and (b) showed the SAD pattern and TEM bright-field image of the Hf films after irradiation at a dose of 4×10^{14} Xe^+/cm^2 by 200 KeV xenon ions. The SAD pattern of the irradiated Hf films can easily be identified to be an fcc structure with the lattice constant of 4.32 Å and the corresponding index results were listed in Table 4. Upon further irradiation to some higher doses, the Hf film remained in the fcc structure. The structural phase transition observed in the Hf film can be summarized as follows:

$$\text{as-deposited hcp Hf} \overset{4\times10^{14}\ Xe^+/cm^2}{\longrightarrow} \text{fcc Hf}$$

The above structural phase transition observed in xenon ion irradiated Hf film suggested that the energy barrier between hcp Hf and fcc Hf should be very low, and the difference of the cohesive energies of the fcc and hcp structures should be small, which is in agreement with the above *ab initio* results.

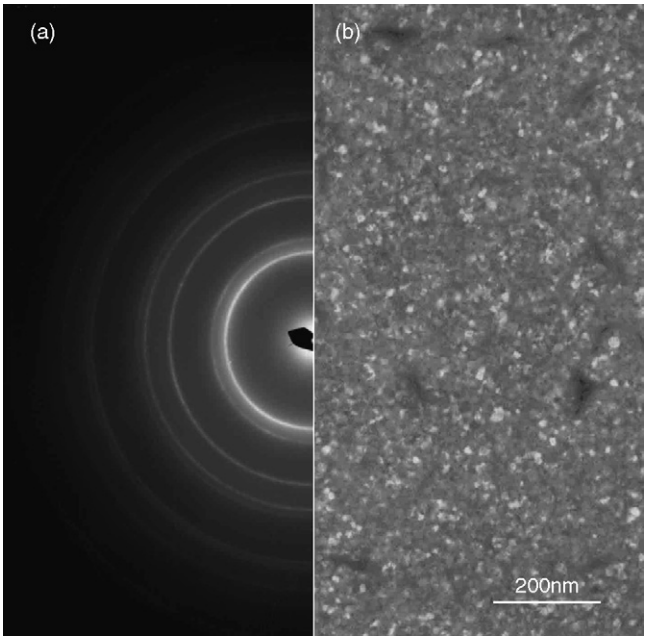

Fig. 4. (a) The SAD pattern of an fcc structure. (b) The corresponding TEM bright-field image of the irradiated Hf film by 200 keV xenon ions with a dose of 4×10^{14} Xe^+/cm^2.

Table 4
Indexing of the fcc structure in the irradiated Hf films at a dose of 4×10^{14} Xe^+/cm^2

D_{exp} (Å)	hkl	D_{cal} (Å)
2.49	111	2.49
2.16	200	2.16
1.53	220	1.53
1.30	311	1.30
1.25	222	1.25
1.08	400	1.08

$a = 4.32$ Å.

As mentioned above, the cohesive energies of both fcc and hcp structures were calculated to have very minor difference, i.e. $(-9.7333) - (-9.8029) = 0.0696$ eV, which can easily be overcome by the 200 keV xenon ion irradiation through atomic collision.

Moreover, concerning the growth kinetics, fcc and hcp are similar structures in which the atomic configurations are basically identical with only a minor difference in stacking sequence of the most close-packed planes, i.e., ABCABC... for fcc, and ABAB... for hcp structures, respectively. The hcp-to-fcc transition is a fast transition mechanism able to complete during the relaxation period of ion beam mixing. Consequently, the lattice adjustment to transform hcp to fcc is geometrically simple, and a fast sliding of the atoms in $(0\,0\,0\,1)_{hcp}$ planes along various $\langle 1\,\bar{1}\,0\,0\rangle$ directions by a vector of $\frac{1}{6}\langle 1\,\bar{1}\,0\,0\rangle$ can readily realize such a structural phase transition. The crystallographic relationship is $[1\,\bar{1}\,0\,0]_{hcp}||[1\,1\,\bar{2}]_{fcc}$, which results in a lattice parameter relationship as $a_{fcc} = \sqrt{2}a_{hcp}$ and $a_{fcc} = \frac{\sqrt{3}}{2}c_{hcp}$. In our experiment, the lattice parameters of the hcp structures in the as-deposited pure Hf films were identified to be $a = 3.19$ and $c = 5.17$ Å. According to the growth kinetics, the parameters of the fcc phase could be deduced from the hcp phase to be around $a_{fcc} \approx 4.50$ Å, which was approximately compatible with those of the formed fcc phases in the irradiated films, i.e., $a_{fcc} = 4.32$ Å within an error range about 5%. Fig. 5 shows the mechanism of the hcp-to-fcc transition.

3.3. Structural phase transition in the Hf–Ni–Hf film

Fig. 6(a) and (b) showed the SAD pattern and TEM bright-field image, respectively of the as-deposited Hf–Ni sandwich-structured film consisting of two Hf layers and one Ni layer. From the figure, two sets of fcc structures were identified and their lattice constants were indexed to be 4.21 and 3.86 Å, which could refer to the lattice parameters of the fcc-Hf and the fcc-Ni phases, respectively. Table 5 lists the crystallographic indexing results from the SAD pattern. The Hf–Ni sandwich-structured film was also analyzed by the Rutherford backscattering spectrometry (RBS) with 2.0 MeV He ions at a 165° scattering angle to confirm the monolayer relative thickness of the as-deposited film. Fig. 7 showed the observed spectrum from RBS and the simulated spectrum of the sandwich-structured film from SIMNRA software [15], respectively. From the observed and the simulated spectra, it can be found the Hf peak was separated

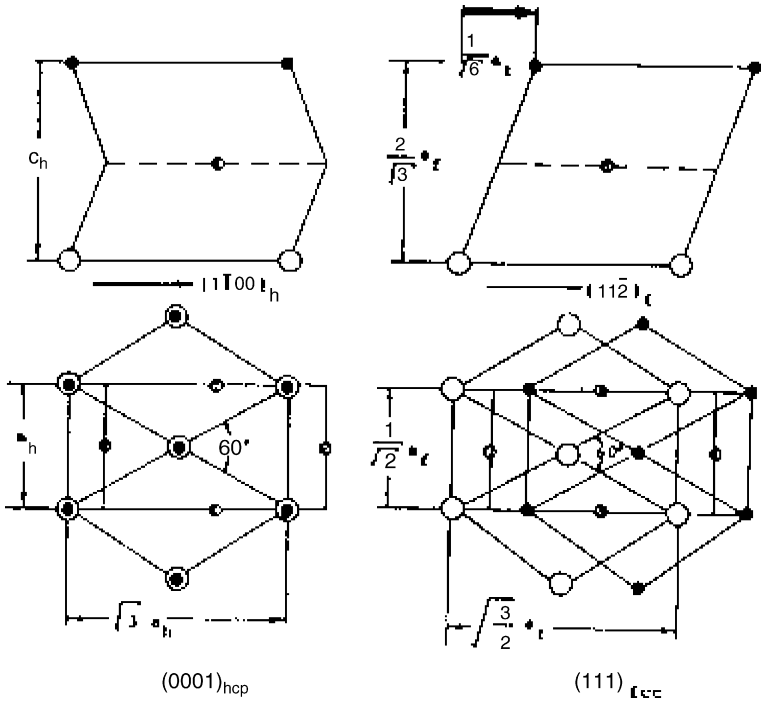

Fig. 5. The crystal growth mechanism of the hcp-to-fcc transition. The sliding plane is $(0\,0\,0\,1)_{hcp}$ in hcp structure along the $\frac{1}{6}\langle 1\,\bar{1}\,0\,0\rangle$ sliding vector.

into two peaks, which represented two individual Hf layers, i.e., the as-deposited film was well kept in its designed sandwich-structured configuration. Besides this, from the simulated spectrum, both the Hf and Ni layers can be estimated to be about 180 and 40 Å, respectively, by simulation using the SIMNRA software [15]. The overall composition of Ni and Hf constituents in the sandwich-structured film was confirmed by the PLASMA-SPEC-I inductive coupled plasma atomic emission spectrum (ICP) to be about 24.3% and 75.7% respectively with a measuring error of 6%.

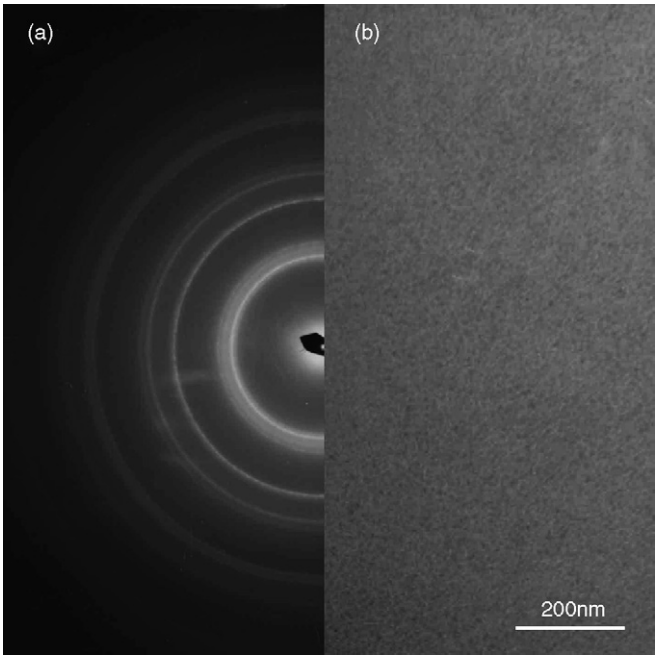

Fig. 6. (a) The SAD pattern of two fcc structures. (b) The corresponding TEM bright-field image of the as-deposited Ni–Hf sandwich-structured film.

The SAD pattern of the as-deposited Ni–Hf film was identified to be two fcc structures with the lattice constants of 3.86 and 4.21 Å, respectively. It indicated that the lattice structure of the Hf monolayer was changed to be an fcc structure and its lattice constant had been reduced (compared with that of α-Hf) while that of the Ni lattice structure was enlarged. It is an interesting issue that the pure Hf film is in an hcp structure, while it easily changes into an fcc structure when a thin Ni layer is embedded in between of the two Hf layers, resulting in changing of the lattice constants of the two metals. It is reasonably assumed that the middle Ni layer induced some interfacial energy or residual stress into the Ni–Hf sandwich-structured film and possibly caused an hcp-to-fcc structural phase transition in the two Hf layers. Compared with the *ab initio* calculation results and the crystal growth kinetics discussed above, the hcp-

Table 5
the indexing results of two fcc structures in the as-deposited Ni–Hf films

D_{exp} (Å)	*h k l* for fcc-Hf	*h k l* for fcc-Ni	D_{cal} (Å)
2.46	1 1 1		2.43
2.23		1 1 1	2.23
2.14	2 0 0		2.11
1.51	2 2 0		1.49
1.28	3 1 1		1.27
1.23	2 2 2		1.22
0.97	3 3 1		0.97
0.94	4 2 0		0.94
0.86	4 2 2		0.86
0.81	3 3 3		0.81
0.75		3 3 3	0.74

$a = 4.21$ Å for fcc-Hf and $a = 3.86$ Å for fcc-Ni.

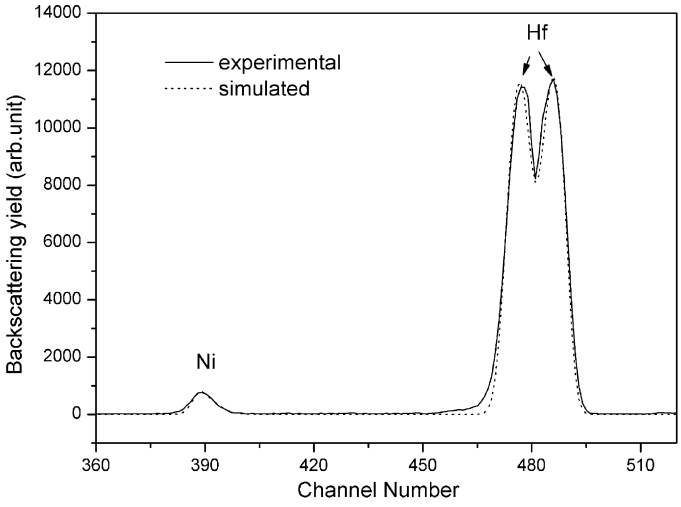

Fig. 7. RBS and its simulated spectrums of the Ni–Hf sandwich-structured layer. The solid line is for the experimental data and the dot line is for the simulated results for the sandwich structure.

to-fcc structural phase transition confirmed a small difference of the cohesive energies and the similar configurations of the hcp and fcc structures of the pure hafnium. However, this interesting issue certainly deserves much further theoretical and experimental studying and explanations.

Fig. 8(a) and (b) showed the SAD pattern and TEM bright-field image of the Ni–Hf sandwich-structured film, respectively, after irradiation by 200 keV xenon ions to a dose of 4×10^{14} Xe^{+}/cm^{2}. From the figure, a uniform fcc crystalline structure was indexed and its lattice constant was confirmed to be 4.18 Å with a measuring error of about 5%. It is of interest to note that the structure of the Ni–Hf film has changed into a unique fcc structure by ion irradiation.

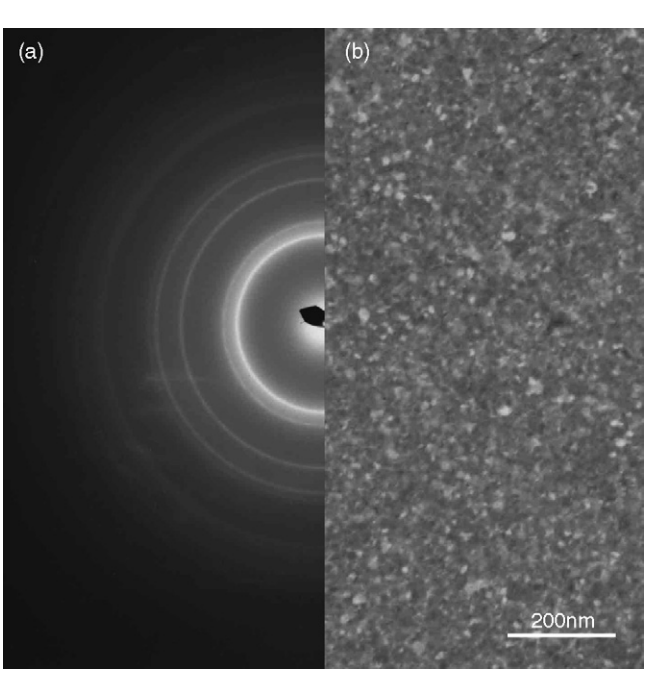

Fig. 8. (a) The SAD pattern of an fcc structure. (b) The corresponding TEM bright-field image of the irradiated Ni–Hf film at a dose of 4×10^{14} Xe^{+}/cm^{2}.

Referring again to the *ab initio* calculation results, it is predicted that the fcc-type structures (A15 and $L1_2$ structures) for the Hf-rich alloy ($Ni_{25}Hf_{75}$) have the lower total energies than both the mechanical mixture (75% fcc-Hf and 25% fcc-Ni) and the hcp-type structures ($D0_{19}$), suggesting that the cubic-type structures were more likely to be formed than the mixture and hexagonal counterpart, which is in agreement with the resultant fcc-type structure in experimental observation. Moreover, the lattice constant of the fcc structure in the irradiated film was identified to be $a = 4.18$ Å, which is quite close to that of the $L1_2$ structure (fcc-type) in the *ab initio* calculation. It should be noted that the SAD pattern of the irradiated Ni–Hf film with the composition of $Ni_{25}Hf_{75}$ confirmed an fcc structure, which is not exactly the ordered $Ni_{25}Hf_{75}$ fcc structure required in VASP calculation, however, it confirms the existence of such a possible state locating near $Ni_{25}Hf_{75}$ with a structure of fcc-type in the Ni–Hf system.

In summary, the structural phase transition in the Ni–Hf sandwich-structured film can be summarized as follows:

$$\mathrm{NiHf} \xrightarrow{\text{as-deposited}} \text{fcc-Hf}\,(a = 4.21\ \text{Å}) + \text{fcc-Ni}\,(a = 3.86\ \text{Å}) \xrightarrow{4\times10^{14}\ \mathrm{Xe^{+}/cm^{2}}} \text{fcc}\,(a = 4.18\ \text{Å})$$

4. Concluding remarks

1. An hcp-to-fcc structural phase transition was observed in pure Hf films upon xenon ion irradiation and could be attributed to a small energy difference between the hcp and fcc structures known from *ab initio* calculations. Kinetically, the fast transition mechanism of the hcp-to-fcc transition is due to the similar configuration of the two structures.
2. Two fcc crystalline structures were identified in the as-deposited sandwich-structured Hf–Ni–Hf sample, and a uniform fcc structure was obtained after xenon ion irradiation. Such an fcc-type structure (i.e., $L1_2$ structure) was predicted by *ab initio* calculation to be metastable near the composition of $Ni_{25}Hf_{75}$, and the prediction was in agreement with the above experimental observation.

Acknowledgements

The authors are grateful to the financial support from the National Natural Science Foundation of China, The Ministry of Science and Technology of China (G20000672), and the Administration of Tsinghua University.

References

[1] B.X. Liu, W.S. Lai, Q. Zhang, Mater. Sci. Eng. R29 (2000) 1.
[2] M.W. Thompson, Defects and Radiation Damage in Metals, Cambridge University Press, Cambridge, England, 1969 (Chapters 4–5).
[3] X. He, X.Y. Li, B.X. Liu, J. Phys. Soc. Japan 72 (2003) 12.
[4] Z.C. Li, D.P. Yu, B.X. Liu, Phys. Rev. B 65 (2002) 24.
[5] F.R. De Boer, R. Boom, W.C.M. Mattens, A.R. Miedema, A.K. Niessen, Cohesion in Metals: Transition Metal Alloys, North-Holland, Amsterdam, 1989.
[6] O. Jin, B.X. Liu, Mater. Lett. 27 (1996) 165.

[7] J.H. Li, H.B. Guo, B.X. Liu, Acta Mater. 53 (2005) 743.
[8] G. Kresse, J. Hafner, Phys. Rev. B 47 (1993) 558.
[9] G. Kresse, J. Furthmüller, Comput. Mater. Sci. 6 (1996) 15.
[10] G. Kresse, J. Furthmüller, Phys. Rev. B 54 (1996) 11169.
[11] D. Vanderbilt, Phys. Rev. B 41 (1990) 7892.
[12] J.P. Perdew, Y. Wang, Phys. Rev. B 45 (1992) 13244.
[13] H.J. Monkhorst, J.D. Pack, Phys. Rev. B 13 (1976) 5188.
[14] J.F. Ziegler, J.P. Biersack, U. Littmark, The Stopping and Range of Ions in Solids, Pergamon Press, New York, 1985.
[15] M. Mayer, SIMNRA, a simulation program for the analysis of NRA, RBS and ERDA, in: J.L. Duggan, I.L. Morgan (Eds.), Proceedings of the 15th International Conference on the Application of Accelerators in Research and Industry, American Institute of Physics Conference Proceedings 475, 1999, p. 541.